Ultrasonics/Baron Propagation of elastic waves in an anisotropic functionally graded hollow cylinder in vacuum

Cécile Baron*,a,b

[a] *UPMC Univ Paris 06, UMR 7190, Institut Jean Le Rond d'Alembert, F-75005 Paris, France.*
[b] *CNRS, UMR 7190, Institut Jean Le Rond d'Alembert, F-75005 Paris, France.*

Abstract

As a non-destructive, non-invasive and non-ionizing evaluation technique for heterogeneous media, the ultrasonic method is of major interest in industrial applications but especially in biomedical fields. Among the unidirectionally heterogeneous media, the continuously varying media are a particular but widespread case in natural materials. The first studies on laterally varying media were carried out by geophysicists on the Ocean, the atmosphere or the Earth, but the teeth, the bone, the shells and the insects wings are also functionally graded media. Some of them can be modeled as planar structures but a lot of them are curved media and need to be modeled as cylinders instead of plates. The present paper investigates the influence of the tubular geometry of a waveguide on the propagation of elastic waves. In this paper, the studied structure is an anisotropic hollow cylinder with elastic properties (stiffness coefficients c_{ij} and mass density ρ) functionally varying

*Corresponding author
Email address: cecile.baron@upmc.fr (Cécile Baron)

in the radial direction. An original method is proposed to find the eigenmodes of this waveguide without using a multilayered model for the cylinder. This method is based on the sextic Stroh's formalism and an analytical solution, the matricant, explicitly expressed under the Peano series expansion form. This approach has already been validated for the study of an anisotropic laterally graded plate (Baron et al., 2007a; Baron and Naili, 2010). The dispersion curves obtained for the radially-graded cylinder are compared to the dispersion curves of a corresponding laterally-graded plate to evaluate the influence of the curvature.

Preliminary results are presented for a tube of bone in vacuum modelling the *in vitro* conditions of bone strength evaluation.
Key words:
elastic wave propagation, radially graded tube, Stroh's formalism,
waveguide, *in vitro* bone characterization

---

1. Introduction

The observation of natural media and particularly of living tissues is a great source of inspiration for scientists. As an example, they develop industrial Functionally Graded Materials (FGM) in the 80's which reproduce a characteristic observed in natural media such as wood, bone or shells. The continuous variation of the mechanical properties of these materials reveals interesting mechanical behavior particularly exploited in high-technology and biomedical applications (Watari et al., 2004; Hedia and Mahmoud, 2004; Lin et al., 2009). As a consequence, the non-destructive characterization of FGM structures became a key issue: first, to better understand the nat-

ural mechanisms observed and second, to guide the conception of groundbreaking FGM. Surface and guided waves are significant information source in non-destructive testing and evaluation of complex structures. A lot of works detailed the behavior of the guided waves in isotropic or anisotropic plates (Rayleigh, 1885; Lamb, 1917; Viktorov, 1970; Auld, 1973). Also, elastic wave propagation in cylindrical structures formed from material with lower anisotropy than orthotropy has been the subject of numerous theoretical and experimental investigations widely published (Mirsky, 1965; Zemanek, 1972; Honarvar et al., 2007). For anisotropic material, the complexity of the problem relies on the fact that the boundary problem do not permit solution in cylindrical functions except in some particular configurations (Mirsky, 1964).

In this work, we solve the wave equation in an anisotropic waveguide with one-direction heterogeneity using a general method based on the sextic Stroh's formalism (Stroh, 1962). It takes into account the unidirectional continuous variation of the properties of the waveguide without using a multilayered model. It is based on the knowledge of an analytical solution of the wave equation, the matricant, explicitly expressed *via* the Peano series expansion. The accuracy of the numerical evaluation of this solution and its validity domain are perfectly managed (Baron, 2005; Youssef and El-Arabawi, 2007). One of the advantages of knowing an analytical solution with respect to purely numerical methods is to control all the physical parameters and to interpret more easily the experimental data which result from the interaction and coupling of numerous physical phenomena.

In this paper, a sample of long bone is considered as an example of anisotropic functionally graded tube. The material is multiscale and the dis-

crete variations of its microscopic properties (bone matrix elasticity, micro-architecture etc.)(Bousson et al., 2001; Bensamoun et al., 2004; Saïed et al., 2008) is assumed to induce continuous profiles of macroscopic properties in the radial direction (Baron et al., 2007b; Haiat et al., 2009; Baron and Naili, 2010). Obviously, the mechanical behavior of bone depends on several parameters (microstructure, elasticity and geometry). The curvature is part of them and its influence remains unclear.

We first present the method and its setup for the cylindrical waveguide; this method has been validated by comparing our results to the dispersion curves obtained from classical schemes on homogeneous and functionally graded waveguides. Some advantages of the method are underlined: i) general anisotropy may be taken into account for cylindrical structures; ii) the influence of the property gradient on the mechanical behavior of the waveguide may be investigated; iii)the influence of the curvature on the propagation of elastic waves may be evaluated.

2. Method

We consider an elastic tube of thickness t placed in vacuum.

The radius r varies from a_0 to a_q, respectively the inner and outer radius of the tube (Figure 1). The elastic cylinder is supposed to be anisotropic and is liable to present continuously varying properties along its radius ($\mathbf{e}_r$-axis). These mechanical properties are represented by the stiffness tensor $\mathbb{C} = \mathbb{C}(r)$ and the mass density $\rho = \rho(r)$.

2.1. System equations

The momentum conservation equation associated with the constitutive law of linear elasticity (Hooke's law) gives the following equations:

$$\begin{cases} \mathrm{div}\boldsymbol{\sigma} = \rho\dfrac{\partial^2\mathbf{u}}{\partial t^2}, \\ \boldsymbol{\sigma} = \dfrac{1}{2}\mathbb{C}\,(\mathrm{grad}\mathbf{u} + \mathrm{grad}^T\mathbf{u}), \end{cases} \tag{1}$$

where $\mathbf{u}$ is the displacement vector and $\boldsymbol{\sigma}$ the stress tensor.

We are seeking the solutions of wave equation for displacement ($\mathbf{u}$) and radial traction vector ($\boldsymbol{\sigma}_r = \boldsymbol{\sigma}.\mathbf{e}_r$) expressed in the cylindrical coordinates (r, θ, z) with the basis $\{\mathbf{e}_r, \mathbf{e}_\theta, \mathbf{e}_z\}$:

$$\begin{aligned} \mathbf{u}(r,\theta,z;t) &= \mathbf{U}^{(n)}(r)\exp\imath\,(n\theta + k_z z - \omega t)\,, \\ \boldsymbol{\sigma}_r(r,\theta,z;t) &= \mathbf{T}^{(n)}(r)\exp\imath\,(n\theta + k_z z - \omega t)\,; \end{aligned} \tag{2}$$

with k_z the axial wavenumber and n the circumferential wavenumber.
We distinguish two types of waves propagating in a cylindrical waveguide: the *circumferential waves* and the *axial waves*. The *circumferential waves* are the waves traveling in planes perpendicular to the axis direction. They correspond to $u_z(r) = 0\,(\forall r)$, $k_z = 0$ and $n = k_\theta a_q$. The *axial waves* are the waves traveling along the axis direction, the circumferential wavenumber is an integer $n = 0, 1, 2, ...$ Among the *axial wave*s, we distinguish three types of modes numbered with two parameters (n, m) representing the circumferential wavenumber and the order of the branches: longitudinal (L), flexural (F) and torsional (T) modes. The longitudinal modes are axially symmetric ($n = 0$), they are noted $L(0, m)$ and sometimes called the breathing modes (Auld, 1973). For the two other types of modes, two classifications have

been proposed in the literature. Meitzler (Meitzler, 1961) and Zemanek (Zemanek, 1972), following Gazis work (Gazis, 1959), restricted the T-modes to axially symmetric circumferential fundamental modes $T(0, m)$ and the modes with non-zero n are considered as F-modes $F(n, m)$. An other way is proposed by Nishino and colleagues (Nishino et al., 2001) who considered that the n-parameter of the T-modes is not limited to zero. Consequently they can associate "their" L- and F- modes to the Lamb waves (coupled bulk longitudinal and bulk shear-vertical waves) in the plate and the T-modes to the bulk horizontal-shear waves propagating in the plate. This classification may be relevant in the case of isotropic media but it becomes invalid for anisotropic media for which the flexural waves are longitudinal shear waves (Gazis, 1959).

In this paper, only the *axial waves* are investigated and the usual classification of Gazis (Gazis, 1959) is used.

2.2. A closed-form solution: the matricant

Introducing the expression (2) in the equation (1), we obtain the wave equation under the form of a second-order differential equation with non-constant coefficients. In the general case, there is no analytical solution to the problem thus formulated. The most current methods to solve the wave equation in unidirectionally heterogeneous media are derived from the Thomson-Haskell method (Thomson, 1950; Haskell, 1953). These methods are appropriate for multilayered structures (Kenneth, 1982; Lévesque and Piché, 1992; Wang and Rokhlin, 2001; Hosten and Castaings, 2003). But, for continuously varying media, these techniques mean to replace the continuous profiles of properties by step-wise functions. Thereby the studied problem

becomes an approximate one, even before the resolution step; the accuracy of the solution as its validity domain are hard to evaluate. Moreover, the multilayered model of the functionally graded waveguide creates some "virtual" interfaces likely to induce artefacts. Lastly, for generally anisotropic cylinders, the solutions cannot been expressed analytically even for homogeneous layers (Mirsky, 1964; Nelson et al., 1971; Soldatos and Jianqiao, 1994).

In order to deal with the exact problem, that is to keep the continuity of the properties variation, the wave equation is written under the sextic Stroh's formalism (Stroh, 1962) in the form of an ordinary differential equations system with non-constant coefficients for which an analytical solution exists: the matricant (Baron, 2005). Another method relies on the Legendre's polynomial as explained and used in (Lefebvre et al., 2002; Elmaimouni et al., 2003, 2005, 2008).

Hamiltonian form of the wave equation. In the Fourier domain, the wave equation may be written as:

$$\frac{d}{dr}\boldsymbol{\eta}(r) = \frac{1}{r}\mathbf{Q}(r)\boldsymbol{\eta}(r). \tag{3}$$

The components of the state-vector $\boldsymbol{\eta}(r)$ are the three components of the displacement and the three components of the stress traction in the cylindrical coordinates, and the matrix $\mathbf{Q}(r)$ contains all the information about the heterogeneity: it is expressed from stiffness coefficients of the waveguide in the cylindrical coordinates and from the two acoustical parameters: axial or circumferential wavenumbers (k_z, or n) and the angular frequency ω. The detailed expression of $\mathbf{Q}(r)$ is given in appendix A for the case of a material with orthorhombic crystallographic symmetry but it can be expressed for any

type of anisotropy (Shuvalov, 2003).

Explicit solution: the Peano expansion of the matricant. The wave equation thus formulated has an analytical solution expressed between a reference point (r_0, θ, z) and some point of the cylinder (r, θ, z). This solution is called the matricant and is explicitly written under the form of the Peano series expansion:

$$\mathbf{M}(r, r_0) = \mathbf{I} + \int_{r_0}^{r} \mathbf{Q}(\xi) d\xi + \int_{r_0}^{r} \mathbf{Q}(\xi) \int_{r_0}^{\xi} \mathbf{Q}(\xi_1) d\xi_1 d\xi + ..., \tag{4}$$

where $\mathbf{I}$ is the identity matrix of dimension $(6, 6)$. If the matrix $\mathbf{Q}(r)$ is bounded in the study interval, these series is always convergent (Baron, 2005). The components of the matrix $\mathbf{Q}$ are continuous in r and the study interval is bounded (thickness of the waveguide), consequently the hypothesis is always borne out. The matricant verifies the propagator property (Baron, 2005):

$$\boldsymbol{\eta}(r) = \mathbf{M}(r, r_0)\boldsymbol{\eta}(r_0). \tag{5}$$

Free boundary conditions. The cylinder is supposed to be in vacuum, so the traction-vector $\boldsymbol{\sigma}_r$ defined in (2) is null at both interfaces. Using the propagator property of the matricant through the thickness of the cylinder, the equation (5) is written as $\boldsymbol{\eta}(a_q) = \mathbf{M}(a_q, a_0)\boldsymbol{\eta}(a_0)$:

$$\begin{pmatrix} \mathbf{u}(r = a_q) \\ \mathbf{0} \end{pmatrix} = \begin{pmatrix} \mathbf{M}_1 & \mathbf{M}_2 \\ \mathbf{M}_3 & \mathbf{M}_4 \end{pmatrix} \begin{pmatrix} \mathbf{u}(r = a_0) \\ \mathbf{0} \end{pmatrix}. \tag{6}$$

Equation (6) has non-trivial solutions for $\det\mathbf{M}_3 = 0$. As detailed in appendix A for an orthotropic material and from the equation (4), the components of $\mathbf{M}_3$ are bivariate polynomials in (k_z, ω). Consequently, to seek

out the zeros of det$\mathbf{M}_3$ corresponds to find the couples of values (k_z, ω) which describe the dispersion curves.

3. Results

To calculate the dispersion curves, we evaluate numerically the matricant $\mathbf{M}(a_q, a_0)$ from the expression (4). This step requires us to truncate the Peano series and to numerically calculate the integrals. Thus, the error can be estimated and controlled (Baron, 2005). For the calculations in the plate we retained 70 terms in the series and evaluate the integrals over 100 points using the Simpson's rule (fourth-order integration method) and for the tube, we retained 33 terms in the series and evaluate the integrals over 30 points. These choices are not optimized but ensure the convergence of the solution and the accuracy of the results in the range of frequency-thickness products considered for a reasonable computation time (few dozen of minutes on a desktop computer).

3.1. Validation

We compare our results to results from the literature obtained on homogeneous tubes (Mirsky, 1965; Nishino et al., 2001) (not shown). In the following part, the method is validated calculating the dispersion curves obtained for an isotropic FGM cylinder previously studied in the literature (Han et al., 2002; Elmaimouni et al., 2003, 2005). The properties of the tube (Young's modulus E, Poisson's ratio ν and mass density ρ) vary from silicon nitride properties at the inner interface ($r = a_0$) to the properties of stainless steel at the outer interface ($r = a_q$). The values of the properties for these two

materials are reported in Table 1.

The dispersion curves are compared for an affine profile:

$$\begin{aligned} E(r) &= E_{out} + (E_{in} - E_{out})\,(r - a_0)/(a_q - a_0); \\ \nu(r) &= \nu_{out} + (\nu_{in} - \nu_{out})\,(r - a_0)/(a_q - a_0); \\ \rho(r) &= \rho_{out} + (\rho_{in} - \rho_{out})\,(r - a_0)/(a_q - a_0). \end{aligned} \tag{7}$$

On Figure 2, the dispersion curves obtained for an isotropic FGM tube (Table 1) from two different schemes, Peano expansion of the matricant and Legendre polynomials, are in perfect agreement.

3.2. Influence of the ratio t/a_q

As mentioned in (Protopappas et al., 2006) and shown in (Lefebvre et al., 2002), when the outer radius of the tube a_q is large compared to the wall thickness t, the longitudinal modes are very close to the Lamb modes obtained for a plate of the same thickness. Nishino and colleagues detailed the influence of the ratio t/a_q on the similarity of the modes of the cylindrical waveguide with the Lamb's waves (Nishino et al., 2001). The same trend is observed for the torsionnal modes as pointed in (Nishino et al., 2001): for small values of the ratio t/a_q (typically less than 0.5) they are very similar to horizontal shear waves propagating in a plate of the same thickness. Considering the flexural waves, it is a little more delicate and sometimes cleverly sidestepped. In (Lefebvre et al., 2002), the comparison is not convincing if superimposing the figures (Figures 2, 3 and 4 in (Lefebvre et al., 2002)) and in Protopappas' paper (Protopappas et al., 2006), the comparison is made for particular flexural modes $F(1, 2m + 1)$ $(m = 0, 1, 2)$.

Flexural modes are characterized by a three-dimensionnal polarization vector. As underlined by Rose (Rose, 1999), understanding the physical characteristics of flexural modes is necessary for advanced applications involving wave reflection from defects. For instance it can be difficult experimentally to generate pure longitudinal modes over a given frequency range. So, this point needs clarification.

Homogeneous isotropic tube. In this part, the results are inspired by Nishino's ones for a homogeneous isotropic aluminum tube ($C_L = 6400$ m/s, $C_T = 3040$ m/s, $\rho = 2.7$ kg/m^3). Two configurations are represented: a) $t/a_q = 0.4 < 0.5$; b) $t/a_q \approx 0.7 > 0.5$.

The results reported on Figure 3 and Figure 4 are in agreement with previous experimental and numerical studies above-cited. The dispersion curves obtained for the longitudinal and torsionnal modes are very similar to the plate modes for $t/a_q < 0.5$ except at low frequency-thickness products ($ft < 1$ MHz.mm). When t/a_q increases the discrepancy becomes more and more significant in the whole range of frequency-thickness products.

As underlined before the case of flexural modes is more complex. We observe on Figure 5 that for the first five modes, the branches $F(1, m)$ when m is even are similar to the Lamb's modes, whereas those $F(1, m)$ when m is odd are similar to the SH modes. For higher order modes, it seems that they are partly similar to Lamb's modes and partly similar to SH waves. These results are in accordance with the definition given by Gazis of longitudinal shear waves (Gazis, 1959). Furthermore, the influence of the ratio t/a_q remains identical to what it has been observed for longitudinal and torsional modes.

Heterogeneous anisotropic tube. The same trend is observed for anisotropic homogeneous structures (results not presented) and for anisotropic functionally graded ones. The anisotropic functionally graded structure studied in this paper has the mechanical properties of the cortical bone.

As the great majority of the biological tissue, the cortical bone is a complex medium. It is anisotropic, multi-components, heterogeneous. It can be modeled as a two-phase medium: the bone matrix and the pores full of marrow (assimilated to water). The characteristic size of the pores in the cortical bone is less than a few hundred micrometers. The classical range of frequency used in quantitative ultrasonography to evaluate bone fragility is $[0.2; 2.5]$ MHz. For such frequencies, the wavelength of the ultrasonic waves is larger than the size of the pores and the waves propagate in an effective macroscopic medium whose properties obviously depend on the microscopic properties such as the porosity or the intrinsic material properties of the bone matrix. An increasing number of papers underlined the relevancy of taking into account these heterogeneities accross the cortex to improve the ultrasonic method for cortical bone assessment (Nicholson et al., 2002; Protopappas et al., 2006; Haiat et al., 2009). It may be particularly relevant in the case of healing bone as proposed by Protopappas and colleagues (Protopappas et al., 2006, 2007). In their papers, they pointed also the limitations of the Lamb wave theory when applied to real bones and underlined the relevance of taking into account the tubular geometry and the anisotropy of the long bones.

In our study, at the scale of the wavelength (few millimeters), the cortical bone may be viewed as a functionally graded material as its porosity increases

continuously along the cortical thickness from the periosteal part (soft tissue side) to the endosteal one (marrow side). It is noteworthy that the intrinsic material properties of the bone matrix vary also across the cortical thickness (Saïed et al., 2008) and contribute to the continuous gradient of macroscopic properties.

In a first approach, knowing the relationship between the porosity and the effective material properties (Baron et al., 2007b) (neglecting the intrinsic material properties variation), the gradient of materials properties may be deduced from the gradient of porosity. To the best of our knowledge, we do not know exactly how the porosity varies across the cortical thickness and how it influences the macroscopic mechanical properties. Several studies brought some information on that point (Bousson et al., 2001; Bensamoun et al., 2004). According to these results, one of the simplest realistic profile of properties to take into account seems to be the affine one.

As shown previously (Baron and Naili, 2010), the propagation of ultrasonic waves in the frequency range of clinical measurement is influenced by the gradient of properties encountered in cortical bone modeled as a plate. Therefore, we study the influence of the curvature on the dispersion curves for a transversely isotropic bone material with linearly varying mechanical properties along its radius. A particular attention was paid to assign realistic values to the properties of bone, for this reason we use the data published in (Haiat et al., 2009; Baron and Naili, 2010). The properties profile tested is an affine function:

$$C(r) = C_m + (C_M - C_m)(r - a_0)/(a - q - a_0); \tag{8}$$

the values of C_m and C_M are reported in Table 2.

The dispersion curves of the longitudinal $L(0,m)$, torsional $T(0,m)$ and flexural $F(1,m)$ modes calculated for a radially graded tube of thickness t are compared with the dispersion curves calculated for a plate of the same thickness (Lamb and Shear Horizontal modes). All the results are obtained from the Peano expansion of the matricant (4).

On figures 6, 7 and 8, we can remark the same trend as observed in figures 3, 4 and 5. The dispersion curves of the longitudinal modes L are very similar to Lamb's modes for ratios $t/a_q < 0.5$ except for low frequency-thickness products ($ft < 0.3$ MHz.mm) (Figure 6). Note that the range is smaller than for the isotropic aluminium tube. The differences become significant when the ratio t/a_q increases. We can also compare the dispersion curves of the torsional modes T to the SH modes in a plate of the same thickness (Figure 7). They are represented in Figure 7 for the same range $[0 - 2\text{MHz.mm}]$. Again, the dispersion curves are very similar for low ratios and the difference increases with t/a_q. Concerning the flexural waves, the anisotropy makes the comparison between tube modes and plate modes more difficult. Again, on Figure 8 we observe the coupling between longitudinal and shear waves expressed in the dispersion curves of the flexural modes. The dependence on t/a_q remains the same.

4. Discussion and perspectives

The non-destructive evaluation of cylindrical anisotropic waveguide remains a key issue, particularly for generally anisotropic materials. The method proposed in the present paper allows to solve the wave equation in an anisotropic tube with radially varying properties. From these results

dealing with the direct problem, further work is needed to develop inversion techniques. There are many industrial applications: super heat resistant materials, "smart structures", powder metallurgy and ceramics or the graded-index plastic optical fibers for communications. Among these domains, the improvement of evaluation of biological tissues such as bone and the development of biomimetic materials for bone implants are booming subjects.

The bone evaluation in prospect. The characterization of bone strength remains a major issue particurlarly in the context of osteoporosis diagnosis known as a public health problem. Nowadays it is established that bone fragility does not depend only on bone density but also on geometry, microstructure and elasticity of bone (Nicholson et al., 2002; Griffith and Genant, 2008). Consequently, a lot of works investigate this way in order to provide relevant criteria of bone strength evaluation. The work presented in this paper is altogether part of that perspective. One of the point is to improve the models used to inverse the experimental data. The goal is to select the relevant characteristic parameters which influence the clinical ultrasonic response and to relate them to the bone fragility. In this study, we take into account the anisotropy of the cortical bone, its tubular geometry and its heterogeneity and we evaluate the influence of the curvature on the ultrasound response representative of the mechanical behavior of the bone.

As a preliminary study on the influence of the curvature on *in-vitro* ultrasound characterization of bone, the results presented are promising. But, obviously there are a lot of weaknesses in this study.

First, one of the limitations is the choice of the elastic properties values and their variation accross the cortical thickness. These values are different

from some data given in other papers (Lang, 1970; Ashman, 1984; Pithioux et al., 2002; Baron et al., 2007b) but remain in a realistic range deduced from experimental measurements (Dong and Guo, 2004) and thermodynamical conditions. Moreover they take into account the known anisotropy of cortical bone. Concerning the linear variation of the elastic properties (stiffness coefficients and mass density), it is a basic model which provides a first insight into the effect of multiscale heterogenity of long bone. A recent study (Haiat et al., 2009), Haiat and colleagues inputed the same values and the same profiles of properties in their simulations and obtained a good agreement between their results and former studies. Nevertheless, experimental data are needed to better define the way the microscopic properties (properties and intrinsic bone matrix properties) vary accross the cortical thickness and contribute to the gardient of macroscopic elastic properties.

Second, the dispersion curves are obtained for a free-stress tube. Consequently, another limitation of this work is the absence of surrounding media which obviously influence the clinical measurements and has to be included in a relevant mechanical model (Baron and Naili, 2010; Moilanen et al., 2008). The presence of fluids inside and outside the tube induces significant changes: the appearance of extra fluid modes and some differences in the shape of the tube modes in terms of attenuation and, phase and group velocities (Plona et al., 1992; Aristegui et al., 2001; Moilanen et al., 2008). Moreover the behaviour of the fluid-loaded structure depends on the viscosity of the fluids (Aristegui et al., 2001). Further work is needed to consider the effect of soft tissue and marrow modelling the bone as a fluid-loaded tube. The boundary conditions may be taken into account in the same way as we did for the

plate (Baron and Naili, 2010). The reflection and transmission coefficients for a fluid-loaded anisotropic tube with radially varying properties will be calculated following the same steps as detailed for the plate. Nevertheless, the present work may provide an interesting tool to give support to *in-vitro* studies.

5. Conclusion

In the context of non-destructive evaluation of complex media, the method presented here reveals several advantages to solve the wave equation in graded anisotropic waveguide. First, the formalism used allows to take into account a general anisotropy of the material even in the case of cylindrical geometry. Second, the Peano expansion of the matricant is one of the only method which provides an analytical solution of the exact problem in a functionally graded medium, that is to say without modelling the waveguide as a multilayered medium. Consequently, the accuracy and validity range are managed. Third, the computation time is a few dozen minutes for the structures studied in this paper. Using this method, it has been demonstrated that the trend revealed in the case of isotropic, homogeneous tubes is confirmed in the case of anisotropic heterogeneous tubes: for thickness to outer radius ratios less than 0.5, the plate model seems to be efficient except at low frequency-thickness products. In the particular context of ultrasonic evaluation of bone, further work is needed to analyse the relevance of the anisotropic heterogeneoous tube model. A study will begin to compare different types of properties profiles and gain an insight into the parameters of the profiles which influence predominantly the ultrasonic response. Anyway, using the Stroh's formalism,

one of the point of this method is the possibility of taking into account the anisotropy of the bone tube which has been proven to widely influence the wave propagation. Furthermore, this study gives some clues on the interaction between the ultrasonic waves and a realistic model of long bone under *in vitro* conditions(tubular geometry, radial heterogeneity and anisotropy): the guided modes are more sensitive to the curvature at low frequency-thickness products (at low frequencies and/or for thin bones). Whereas, the guided waves are more sensitive to the variation of properties at higher frequency-thickness products (at high frequencies and/or for thick bones). Now, this gradient may provide a multiparametric evaluation of the bone fragility by assessing pieces of information on the geometry, the structure and the material at a time and may reveal itself a relevant parameter in the diagnosis an the therapeutic following of the osteoporosis. But a question remains: are the ultrasounds sensitive to this gradient? an experimental study is insistently needed to gain insight on that point.

A. Appendix A

Expression of the vector $\boldsymbol{\eta}(r)$ and of the matrix $\mathbf{Q}(r)$ for a material with orthorhombic crystallographic symmetry (9 independent stiffness coefficients). The symbol $\hat{.}$ represents the quantities in the Fourier domain.

$$\boldsymbol{\eta}(r) = \Big(\ \hat{u}_r(r),\ \hat{u}_\theta(r),\ \hat{u}_z(r),\ \imath r\hat{\sigma}_{rr}(r),\ \imath r\hat{\sigma}_{r\theta}(r),\ \imath r\hat{\sigma}_{rz}(r) \ \Big)^T,$$

and

$$\mathbf{Q}(r) = \frac{1}{r} \left(\begin{array}{cc} -\frac{c_{12}}{c_{11}} & -\imath n \frac{c_{12}}{c_{11}} \\ -\imath n & 1 \\ -\imath k_z r & 0 \\ \imath \left(\gamma_{12} - r^2 \rho \omega^2\right) & -n\gamma_{12} \\ n\gamma_{12} & \imath n^2 \gamma_{12} + \imath r^2 \left(k_z^2 c_{44} - \rho\omega^2\right) \\ k_z r \gamma_{23} & \imath n k_z r \left(\gamma_{23} + c_{44}\right) \end{array} \right. \quad ...$$

$$... \quad \left. \begin{array}{cccc} -\imath k_z r \frac{c_{13}}{c_{11}} & -\frac{\imath}{c_{11}} & 0 & 0 \\ 0 & 0 & -\frac{\imath}{c_{66}} & 0 \\ 0 & 0 & 0 & \frac{\imath}{c_{55}} \\ -k_z r \gamma_{23} & \frac{c_{12}}{c_{11}} & -\imath n & -\imath k_z r \\ \imath n k_z r \left(\gamma_{123} + c_{44}\right) & -\imath n \frac{c_{12}}{c_{11}} & -1 & 0 \\ \imath n^2 c_{44} + \imath r^2 \left(k_z^2 \gamma_{13} - \rho\omega^2\right) & -\imath k_z r \frac{c_{13}}{c_{11}} & 0 & 0 \end{array} \right)$$

with $\gamma_{12} = c_{22} - \frac{c_{12}^2}{c_{11}}$; $\gamma_{13} = c_{33} - \frac{c_{13}^2}{c_{11}}$; $\gamma_{23} = c_{23} - \frac{c_{12} c_{13}}{c_{11}}$.

References

Aristegui, C., Lowe, M., Cauley, P., 2001. Guided waves in fluid-filled pipes surrounded by different fluids. Ultrasonics 39, 367–375.

Ashman, R. B., 1984. A continuous wave measurement of the elastic properties of cortical bone. Journal of Biomechanics 17, 349–361.

Auld, B. A., 1973. Acoustic fields and waves in solids. Wiley Interscience, New York.

Baron, C., 2005. Le développement en série de Peano du matricant pour l'étude de la propagation d'ondes en milieux continûment variables - Peano expansion of the matricant to study elastic wave propagation in continuously heterogeneous media. Ph.D. thesis, Université Bordeaux 1, France.

Baron, C., Naili, S., 2010. Propagation of elastic waves in a fluid-loaded anisotropic functionally graded waveguide: Application to ultrasound characterization. Journal of Acoustical Society of America 127, 1307–1317.

Baron, C., Shuvalov, A., Poncelet, O., 2007a. Impact of localized inhomogeneity on the surface-wave velocity and bulk-wave reflection in solids. Ultrasonics 46, 1–12.

Baron, C., Talmant, M., Laugier, P., 2007b. Effect of porosity on effective diagonal stiffness coefficients (c_{ii}) and anisotropy of cortical at 1 MHz: A finite-difference time domain study. Journal of Acoustical Society of America 122, 1810–1817.

Bensamoun, S., Gherbezza, J.-M., de Belleval, J.-F., Ho Ba Tho, M.-C., 2004. Transmission scanning acoustic imaging of human cortical bone and relation with the microstructure. Clinical Biomechanics 19, 639–647.

Bousson, V., Meunier, A., Bergot, C., Vicaut, E., Rocha, M. A., Morais, M. H., Laval-Jeantet, A.-M., Laredo, J.-D., 2001. Distribution of intracortical porosity in human midfemoral cortex by age and gender. Journal of Bone and Mineral Reasearch 16, 1308–1317.

Dong, X. N., Guo, X. E., 2004. The dependence of transversely isotropic elas-

ticity of human femoral cortical bone on porosity. Journal of Biomechanics 37, 1281–1287.

Elmaimouni, L., Lefebvre, J. E., Gryba, T., Zhang, V., 2003. Polynomial method applied to acoustic waves in inhomogeneous cylinders. In: IEEE Ultrasonics Symposium.

Elmaimouni, L., Lefebvre, J. E., Raherison, A., Ratolojanahary, F. E., 2008. Acoustical Guided Waves in Inhomogeneous Cylindrical Materials. Ferroelectrics 372, 115–123.

Elmaimouni, L., Lefebvre, J. E., Zhang, V., Gryba, T., 2005. Guided waves in radially graded cylinders: a polynomial approach. NDT&E International 38, 344–353.

Gazis, D. C., 1959. Three-dimensional investigation of the propagation of waves in hollow circular cylinders. I. Analytical foundation. Journal of Acoustical Society of America 31, 568–573.

Griffith, J. F., Genant, H. K., 2008. Bone mass and architecture determination: state of the art. Best Practice & Research Clinical Endocrinology & Metabolism 22, 737–764.

Haiat, G., Naili, S., Grimal, Q., Talmant, M., 2009. Influence of a gradient of material properties on ultrasonic wave propagation in cortical bone: Application to axial transmission. Journal of Acoustical Society of America 125, 4043–4052.

Han, X., Liu, G. R., Xi, Z. C., Lam, K. Y., 2002. Characteristics of waves in a

functionally graded cylinder. International Journal for Numerical Methods in Engineering 53, 653–676.

Haskell, N. A., 1953. The dispersion of surface waves on multilayered media. Bulletin of the Seismological Society of America 43, 377–393.

Hedia, H., Mahmoud, N., 2004. Design optimization of functionally graded dental implant. Bio-Medical Materials and Engineering 14, 133–143.

Honarvar, F., Enjilela, E., Sinclair, A., Mirnezami, S., 2007. Wave propagation in transversely isotropic cylinders. International Journal of Solids and Structures 44, 5236–5246.

Hosten, B., Castaings, M., 2003. Surface impedance matrices to model the propagation in multilayered media. Ultrasonics 41, 501–507.

Kenneth, E. G., 1982. A propagator matrix method for periodically stratified media. Journal of Acoustical Society of America 73 (1), 137–142.

Lamb, H., 1917. On waves in an elastic plate. Proceedings of the Royal Society of London A. 93, 114–128.

Lang, S. B., 1970. Ultrasonic method for measuring elastic coefficients of bone and results on fresh and dried bovine bones. In: IEEE Transactions on Biomedical Engineering. Vol. 17.

Lefebvre, F., Deblock, Y., Campistron, P., Ahite, D., Fabre, J. J., 2002. Development of a new ultrasonic technique for bone and biomaterials in vitro characterization. Journal of Biomedical Material Research, Part B 63, 441–446.

Lin, D., Li, Q., Li, W., Zhou, S., Swain, M., 2009. Design optimization of functionally graded dental implant for bone remodeling. Composites: Part B 40, 668–675.

Lévesque, D., Piché, L., 1992. A robust transfer matrix simulation for ultrasonic response of multilayered absorbing media. Journal of Acoustical Society of America 92, 452–467.

Meitzler, A. H., 1961. Mode coupling occuring in the propagation of elastic pulses in wires. Journal of the Acoustical Society of America 33, 435–445.

Mirsky, I., 1964. Axisymmetric vibrations of orthotropic cylinders. Journal of the Acoustical Society of America 36, 2106–2112.

Mirsky, I., 1965. Wave propagation in transversely isotropic circular cylinders, Part I: Theory. Journal of the Acoustical Society of America 37, 1016–1026.

Moilanen, P., Talmant, M., Kilappa, V., Nicholson, P. H. F., Cheng, S., Timonen, J., Laugier, P., 2008. Modeling the impact of soft tissue on axial transmission measurements of ultrasonic guided waves in human radius. Journal of the Acoustical Society of America 124, 2364–2373.

Nelson, R., Dong, S., Kalkra, R., 1971. Vibrations and waves in laminated orthotropic circular cylinders. Journal of Sound and Vibration 18, 429–444.

Nicholson, P. H. F., Moilanen, P., Kärkkäinen, T., Timonen, J., Cheng, S., 2002. Guided ultrasonic waves in long bones: modelling, experiment and *in vivo* application. Physiological Measurement 23, 755–768.

Nishino, H., Takashina, S., Uchida, F., Takemoto, M., Ono, K., 2001. Modal analysis of hollow cylindrical guided waves and applications. Japonese Journal of Applied Physics 30 (1), 364–370.

Pithioux, M., Lasaygues, P., Chabrand, P., 2002. An alternative ultrasonic method for measuring the elastic properties of cortical bone. Journal of Biomechanics 35, 961–968.

Plona, T., Sinha, B., Kostek, S., Chang, S.-K., 1992. Axisymmetric wave porpagation in fluid-loaded cylindrical shells. II: Theory versus experiment. Journal of Acoustical Society of America 92, 1144–1155.

Protopappas, V., Fotiadis, D., Malizos, K., 2006. Guided ultrasound wave propagation in intact and healing long bone. Ultrasound in Medicine and Biology 32, 693–708.

Protopappas, V., Kourtis, I. C., Kourtis, L. C., Malizos, K., Massalas, C. V., Fotiadis, D., 2007. Three-dimensional finite element modeling of guided ultrasound wave propagation in intact and healing long bones. Journal of the Acoustical Society of America 121, 3907–3921.

Rayleigh, J. W. S., 1885. On wave propagating along the plane surface of an elastic solid. Proceedings of the London Mathematical Society 7, 4–11.

Rose, J. L., 1999. Ultrasonic waves in solid media. Cambridge University Press, Cambridge.

Saïed, A., Raum, K., Leguerney, I., Laugier, P., 2008. Spatial distribution of anisotropic acoustic impedance assessed by time-resolved 50-MHz scanning

acoustic microscopy and its relation to porosity in human cortical bone. Bone 43, 187–194.

Shuvalov, A., 2003. A sextic formalism for three-dimensional elastodynamics of cylindrically anisotropic radially inhomogeneous materials. Proceedings of the Royal Society of London A. 459, 1611–1639.

Soldatos, K., Jianqiao, Y., 1994. Wave propagation in anisotropic laminated hollow cylinders of infinite extent. Journal of the Acoustical Society of America 96, 3744–3752.

Stroh, A. N., 1962. Steady state problems in anisotropic elasticity. Journal of Mathematics and Physics 41, 77–103.

Thomson, W. T., 1950. Transmission of elastic waves through a stratified solid medium. Journal of Applied Physics 21, 89–93.

Viktorov, I. A., 1970. Rayleigh and Lamb waves. Plenum Press, New York.

Wang, L., Rokhlin, S. I., 2001. Stable reformulation of transfer matrix method for wave propagation in layered anisotropic media. Ultrasonics 39, 413–424.

Watari, F., Yokoyama, A., Omori, M., Hirai, T., Kondo, H., Uo, M., Kawasaki, T., 2004. Biocompatibility of materials and development to functionally graded implant for bio-medical application. Composites Science and Technology 64, 893–908.

Youssef, I., El-Arabawi, H., 2007. Picard iteration algorithm combined with

Gauss-Seidel technique for initial value problems. Applied Mathematics and Computation 190, 345–355.

Zemanek, J. J., 1972. An experimental and theoretical investigation of elastic wave propagation in a cylinder. Journal of the Acoustical Society of America 51, 265–283.

List of figures

List of tables

1. Elastic properties of the materials at the two interfaces of the tube.
2. The minimal and maximal values $[C_m, C_M]$ of each variable corresponding to the realistic range of variation taken from (Baron and Naili, 2010) with $c_{12} = c_{11} - 2c_{66}$. Remember that the correspondence between space directions and index notation is $1 \leftrightarrow r; 2 \leftrightarrow \theta; 3 \leftrightarrow z$.

	E (GPa)	ν	ρ (kg/m^3)
Stainless steel (outer)	207.82	0.317	8166
Silicon nitride (inner)	322.4	0.24	2370

Table 1: Elastic properties of the materials at the two interfaces of the tube.

$c_{11} = c_{22}$ (GPa)	$c_{13} = c_{23}$ (GPa)	c_{33} (GPa)	$c_{44} = c_{55}$ (GPa)	c_{66} (GPa)	ρ (g.cm^{-3})
$[11.8, 25.9]$	$[5.1, 11.1]$	$[17.6, 29.6]$	$[3.3, 5.5]$	$[2.2, 4.4]$	$[1.66, 1.753]$

Table 2: The minimal and maximal values $[C_m, C_M]$ of each variable corresponding to the realistic range of variation taken from (Baron and Naili, 2010) with $c_{12} = c_{11} - 2c_{66}$. Remember that the correspondence between space directions and index notation is $1 \leftrightarrow r; 2 \leftrightarrow \theta; 3 \leftrightarrow z$.

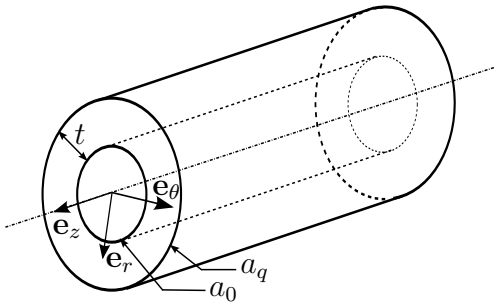

Figure 1: Geometrical configuration of the waveguide.

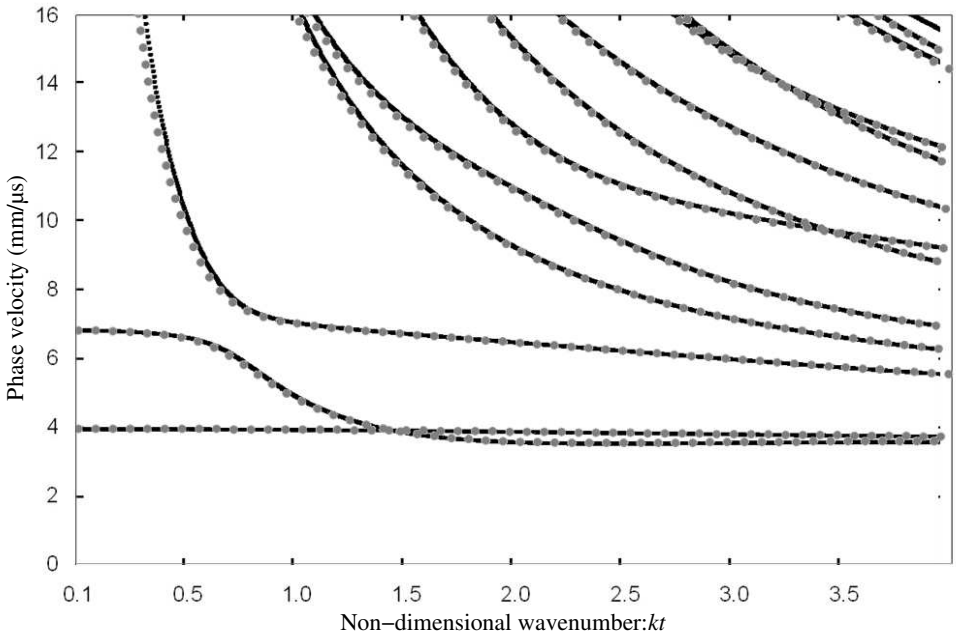

Figure 2: The results obtained from the Stroh's formalism (grey points) compared with the results published in (Elmaimouni et al., 2003) (black points).

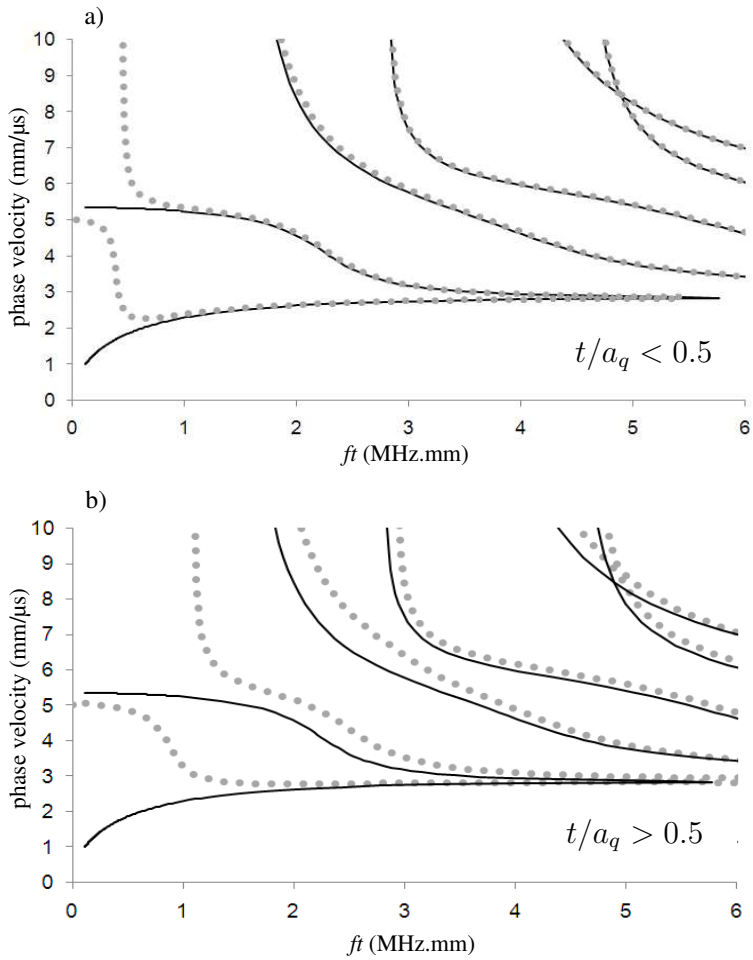

Figure 3: Influence of the ratio t/a_q for a homogeneous isotropic aluminium tube. The Lamb's modes (black lines) are compared with the longitudinal modes $L(0, m)$ (grey points).

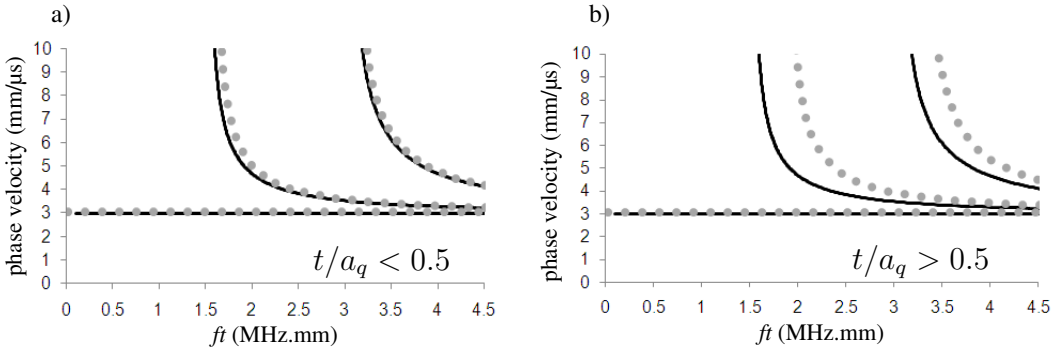

Figure 4: Influence of the ratio t/a_q for a homogeneous isotropic aluminium tube. The SH modes (black lines) are compared with the torsional modes $T(0, m)$ (grey points).

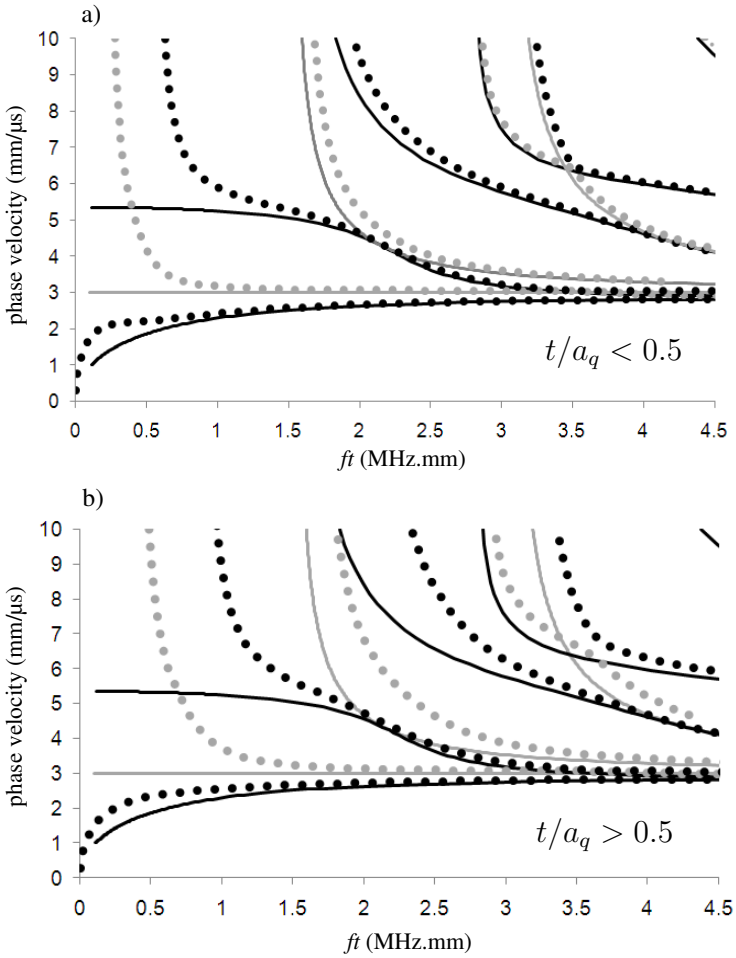

Figure 5: Influence of the ratio t/a_q for a homogeneous isotropic aluminium tube. The SH modes (grey lines) and Lamb's modes (black lines) are compared with the flexural modes $F(1, 2m)$ (grey points) and $F(1, 2m-1)$ (black points) with $m = 1, 2, 3, 4$.

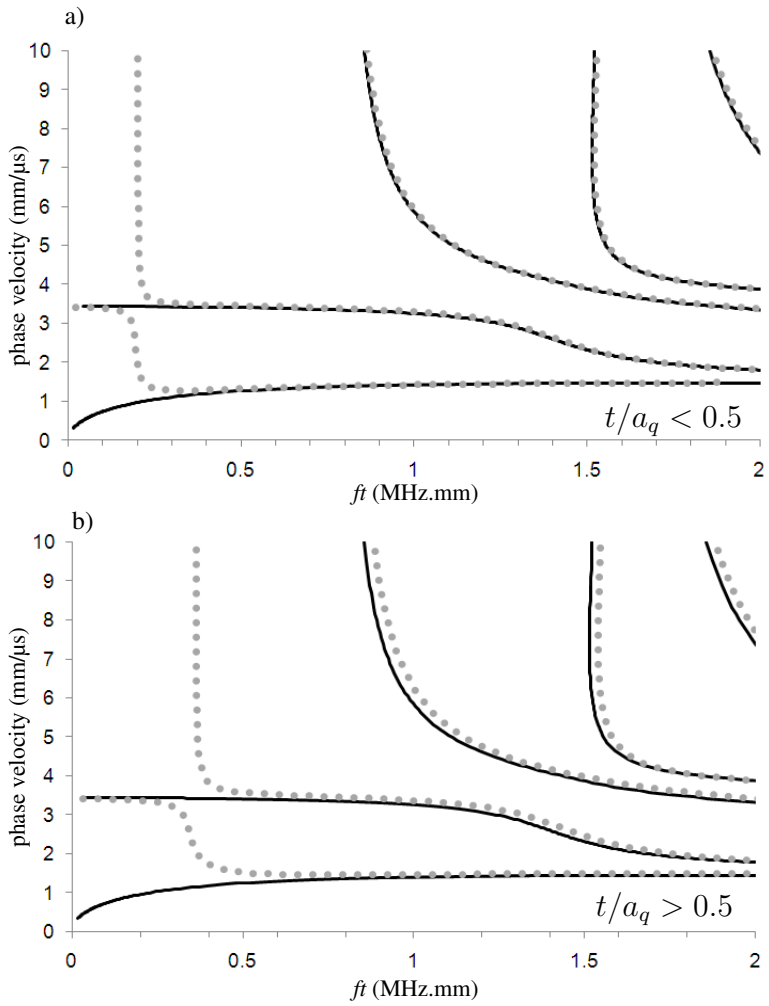

Figure 6: Influence of the ratio t/a_q for a tube with bone properties (Table 2). The Lamb's modes (black lines) are compared with the longitudinal modes (grey circles).

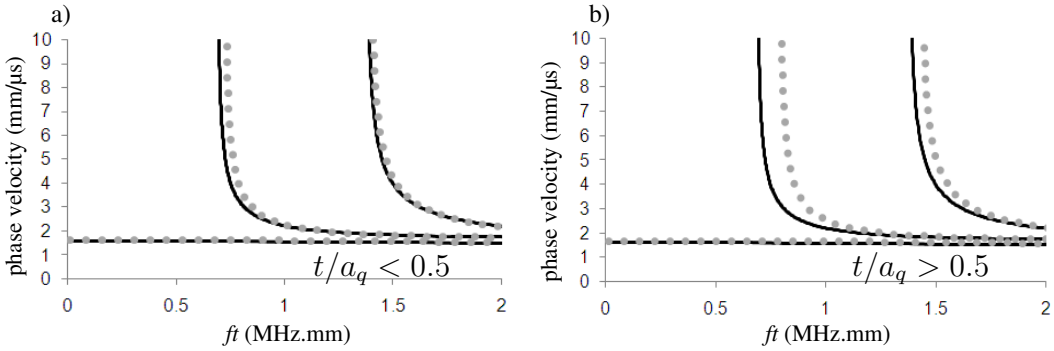

Figure 7: Influence of the ratio t/a_q for a tube with bone properties (Table 2). The SH modes (black lines) are compared with the torsional modes (grey circles).

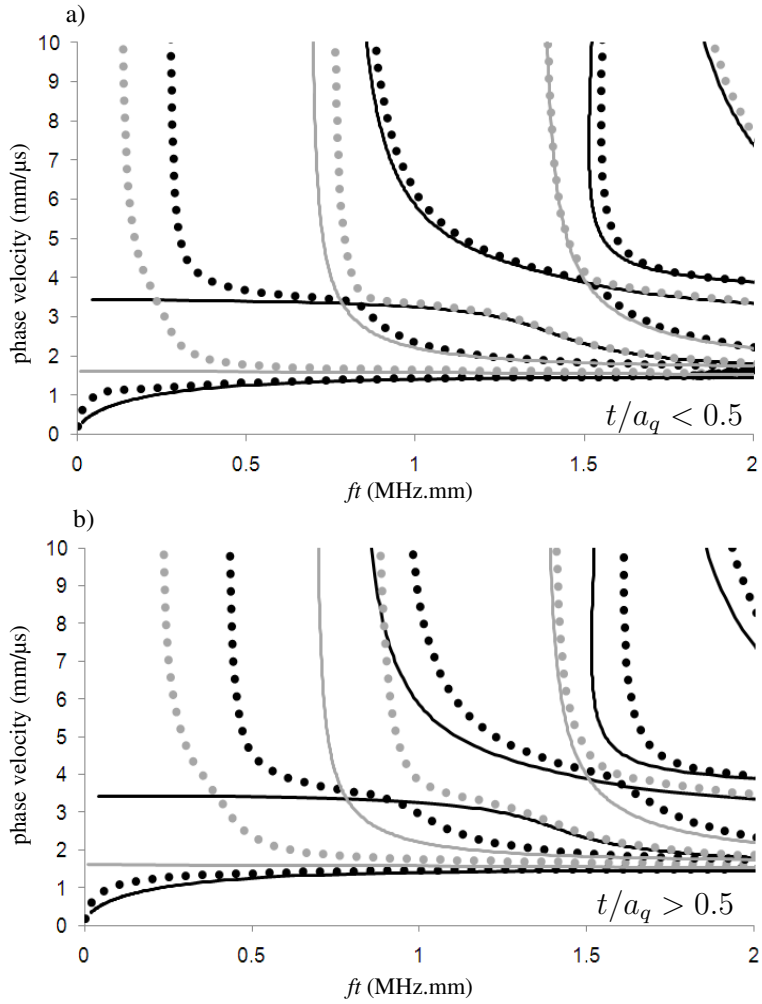

Figure 8: Influence of the ratio t/a_q for a tube with bone properties (Table 2). The SH modes (grey lines) and Lamb's modes (black lines) are compared with the flexural modes $F(1, 2m)$ (grey points) and $F(1, 2m-1)$ (black points) with $m = 1, 2, 3, 4$.